Available online at www.sciencedirect.com
SCIENCE DIRECT®
Carbon 42 (2004) 307–315
CARBON
www.elsevier.com/locate/carbon

The influence of oxidation on the texture and the number of oxygen-containing surface groups of carbon nanofibers

Marjolein L. Toebes, Jürgen M.P. van Heeswijk, Johannes H. Bitter, A. Jos van Dillen, Krijn P. de Jong *

Department of Inorganic Chemistry and Catalysis, Debye Institute, Utrecht University, P.O. Box 80 083, Utrecht 3508 TB, The Netherlands

Received 12 September 2003; accepted 26 October 2003

Abstract

The effect of liquid-phase oxidation on the texture and surface properties of carbon nanofibers has been studied using XRD, TEM, SEM, N_2-physisorption, TGA-MS, XPS and acid–base titrations. Oxidation was performed by refluxing the nanofibers in HNO_3 and mixtures of HNO_3/H_2SO_4 for different times. The graphite-like structure of the treated fibers remained intact, however, the specific surface area and the pore volume increased with the severity of oxidation treatment. For the first time it is shown that the most predominant effect that gives rise to these textural modifications is the opening of the inner tubes of the fibers. Moreover, it is demonstrated that both the total oxygen content (O/C = 0.02–0.07 at/at) as well as the number of acidic groups (1–3 nm^{-2}) are a function of the type of oxidizing agent used and the treatment time. The total oxygen content of the oxidized samples turns out to be substantially higher than can be accommodated in the form of oxygen-containing groups at the exterior surface.

Keywords: A. Carbon fibers, Catalytically grown carbon; B. Oxidation; D. Surface oxygen complexes, Texture

1. Introduction

Carbon materials are widely used, e.g., as adsorbent, as catalyst support and for structural reinforcement of polymers. Main advantages are often their high surface area and chemical inertness. Among the many types of carbons, activated carbon is still the most commonly used. However, more recently, carbon nanofibers (CNF), multi-walled carbon nanotubes (MWNT) [1–3] and related materials have attracted interest. These graphite-like fibers are grown from decomposition of carbon-containing gases on small metal particles. They have unique textural and mechanical properties and contain neither micropores nor impurities.

The hydrophobic and inert nature of the as-grown graphite-like CNF can be unfavorable for some applications. Nevertheless, by treatment in e.g. an oxidizing acid, oxygen-containing surface groups can be introduced thus enhancing the wettability for polar solvents such as water and making the surface more reactive [4–7]. The precise nature of these carbon–oxygen structures is not entirely established, but the results of many reported studies using FT-IR, Boehm-titrations and TPD demonstrate that several types of surface-oxygen groups can be distinguished [4–6]. The number of oxygen-containing surface groups is highly dependent on the way of preparation. A critical survey of methods for the determination of these groups on carbon has been given by Boehm [8]. In contact with aqueous solutions negatively, neutral and positively charged surface sites exist depending on the pH [4].

These oxygen-containing surface groups are formed not only by reaction with oxidizing gases (e.g. O_2, O_3, CO_2) but also by treatment with aqueous solutions of HNO_3, H_2SO_4 or H_2O_2. In this study aqueous solutions of HNO_3 and mixtures of HNO_3/H_2SO_4 have been used. In these solutions the nitronium ion, NO_2^+, is able to attack aromatic compounds, which is probably the first step in the introduction of oxygen-containing surface groups. Therefore the severity of the oxidation treatment depends both on the treatment time and the concentration of NO_2^+, which increases in the order HNO_3 < 1:1 HNO_3/H_2SO_4 < 1:3 HNO_3/H_2SO_4 [7,9,10].

* Corresponding author. Tel.: +31-30-2536-762; fax: +31-30-2511-027.
E-mail address: k.p.dejong@chem.uu.nl (K.P. de Jong).

0008-6223/$ - see front matter © 2003 Elsevier Ltd. All rights reserved.
doi:10.1016/j.carbon.2003.10.036

Over the years the effect of oxidation of classical carbon supports, such as activated carbon, carbon black, graphite and graphite-like materials has been extensively studied. More recently studies on the oxidation of MWNT have been reported [2,7,11–14]. Results show that treatment of MWNT in oxidizing acids results in opening of the inner tubes [11,13,14]. Hoogenraad [2] treated MWNT in HNO_3 to introduce surface oxygen groups, largely carboxylic- or carbonyl groups, to enable the application of Pt- and Pd-complexes via ion-exchange. The iso-electric point (IEP) of 2.3 after treatment was found to be indicative of the presence of carboxylic groups.

Up to now the effect of surface oxidation on the texture and surface properties of fishbone CNF has only scarcely been described. Darmstadt et al. studied the (12 h) oxidation of CNF (diameter $\sim$200 nm) in boiling HNO_3 [15]. They claim that not only the surface became affected; also the ordering of the graphite-like structure in the bulk was decreased. Nonetheless, from the work of Ros et al. where the oxidation treatment of CNF in the liquid-phase (HNO_3, HNO_3/H_2SO_4) had been confined to 2 h it appeared that the macroscopic structure as well as the graphite-like structure of the fibers was preserved [7]. During oxidation, first the formation of carbonyls occurs, which groups are converted into carboxyls and carboxylic anhydrides. Also ether-type oxygen groups in the graphene sheets are formed. Ros et al. [7] stated that the formation of oxygen-containing surface groups occurs mainly at defect sites on the CNF surface. Unfortunately in their work only the total number of oxygen groups is quantified.

Here we report on the effects of surface oxidation of small diameter (20–30 nm) fishbone CNF. XRD, TEM were used to investigate the graphite-like structure of untreated and oxidized CNF. To examine the possible changes in the texture of the CNF N_2-physisorption and SEM were utilized. Moreover TGA-MS, XPS and titrations were used to determine the total oxygen content and the number of acidic surface groups. The thermostability of the surface oxides was studied by titration, TGA-MS and XPS measurements of oxidized samples thermally treated in N_2 at 573, 773 and 973 K.

2. Experimental

2.1. Carbon nanofiber growth

For the growth of CNF, 20 wt.% Ni/SiO_2 was prepared by homogeneous deposition precipitation (HDP) as described by van Dillen et al. [16] using silica (Degussa, Aerosil 200), nickel nitrate (Acros), and urea (Acros). After filtering and washing, the catalyst precursor was dried at 393 K and calcined in static air at 873 K (heating rate 5 K/min) for 2 h.

One gram of the Ni-catalyst precursor was placed in a quartz reactor and prior to the fiber growth reduced in situ for 2 h in a flow of a mixture of H_2 (80 ml/min) and N_2 (320 ml/min) at 1 bar and 973 K (heating rate 5 K/min). Next, the CNF were grown at 823 K in a mixture of CO (80 ml/min), H_2 (28 ml/min), and Ar (292 ml/min) for 24 h. Typically, a CNF yield of 10 g was obtained. A more detailed description of the preparation of the growth catalyst and the growth of the CNF can be found elsewhere [3].

2.2. Surface oxidation of carbon nanofibers

In Table 1 the samples together with their identification codes and the different treatments are listed. After growth all the CNF samples, except for the untreated sample CNF#1, were refluxed for 1 h in a 1 M KOH solution in order to remove the silica support. CNF sample #2 was obtained after subsequent treatment in boiling HCl, to remove exposed nickel metal particles. All the other samples were, after KOH treatment, refluxed in concentrated HNO_3 ($b_p \sim 83$ °C) (#3 and #4) or in a mixture of HNO_3/H_2SO_4 ($b_p \sim 83$–120 °C) (#5 and #6) for different times for activation and for removal of exposed nickel. Typically, 10 g CNF was refluxed in 200 ml KOH or acid. Subsequently, the CNF were washed thoroughly with demi-water and dried in air at 393 K for 16 h.

Table 1
Identification codes, treatment conditions and burn-off (%) of the various carbon nanofiber samples

Code	Base treatment	Acid treatment	N_2 treatment (2 h)	Burn-off (%)
#1	–	–	–	n.d.
#2	Reflux 1 h 1 M KOH	Reflux 1 h conc HCl	–	n.d.
#3	Reflux 1 h 1 M KOH	Reflux 0.5 h conc HNO_3	–	2.4
#4	Reflux 1 h 1 M KOH	Reflux 2 h conc HNO_3	–	3.1
#5	Reflux 1 h 1 M KOH	Reflux 0.5 h conc HNO_3/H_2SO_4 1:1	–	3.7
#6	Reflux 1 h 1 M KOH	Reflux 0.5 h conc HNO_3/H_2SO_4 1:3	–	22.3
#4 573 K N_2	Reflux 1 h 1 M KOH	Reflux 2 h conc HNO_3	573 K	–
#4 773 K N_2	Reflux 1 h 1 M KOH	Reflux 2 h conc HNO_3	773 K	–
#4 973 K N_2	Reflux 1 h 1 M KOH	Reflux 2 h conc HNO_3	973 K	–

n.d. not determined.

2.3. Heat treatment in N_2 of oxidized carbon nanofibers

In order to investigate the thermostability of the oxygen-containing groups on the CNF surface, samples of the CNF oxidized in HNO_3 for 2 h (#4) were heat-treated in flowing nitrogen for 2 h at 573, 773 and 973 K (#4 573, #5 773 and #6 973).

2.4. Carbon nanofiber characterization

Transmission electron microscope (TEM) images were obtained using a Philips CM-200 FEG operated at 200 kV. Samples were prepared by suspending the fibers in ethanol under ultrasonic vibration. Some drops of the thus produced suspensions were brought onto a holey carbon film on a copper grid.

A Philips XL-30 Field Emission Gun (FEG) scanning electron microscope was used to obtain SEM images.

Texture analyses were performed with N_2 physisorption at 77 K, up to a pressure of 1 bar. From the N_2 physisorption data, obtained with a Micromeretics ASAP 2400 apparatus, BET surface area, total mesopore volume and micropore volume (t-plot) were derived. Prior to physisorption measurements, the samples were evacuated at 473 K for at least 16 h.

X-Ray diffraction (XRD) patterns were recorded at room temperature with an Enraf Nonius PDS 120 powder diffractometer system equipped with a position-sensitive detector with a 2θ range of 120° using Co $K\alpha_1$ ($\lambda = 1.78897$ Å) radiation.

The amount of carbon burned-off during oxidation is determined by weighing dried CNF samples before and after the oxidation treatment.

The number of acid sites of the oxidized CNF after the various treatments was determined performing direct acid–base titrations. Since grinding of the mesoporous CNF samples before the titration experiments did not influence the results, it was concluded that transport restrictions did not interfere. Samples of 20–40 mg of untreated and oxidized CNF were stirred with 25 ml of a solution containing 0.1 M NaCl (supporting electrolyte) and 0.1 mM oxalic acid in demi-water, acidified to pH = 3 with HCl. This composition of the solution was found by optimization to give the most reproducible results. While stirring, pure nitrogen was flushed through the reactor and 10 mM NaOH was added dropwise from a buret with a rate of 0.05 ml/min. The pH was monitored using a combined pH electrode PHC 4406. All acid sites with a $pK_a < 7.5$ were measured. It is likely that in the pH range of 3–7.5 only the carboxylic groups are probed. The accuracy of this method was found to be within 10%.

The total number of oxygen-containing groups was measured using thermogravimetric analysis on a Netzsch STA-429 thermobalance. The gases evolved were monitored by a Fisons Thermolab quadropole mass spectrometer, through a capillary situated directly above the sample cup. Samples (20–100 mg) were heated in Ar (60 ml/min) at a rate of 5 K/min to 1123 K.

XPS data were obtained with a Fisons ESCALAB 210I-XL and a Vacuum Generators XPS system. Al $K\alpha$ X-ray radiation was utilized, employing an anode current of 20 mA at 15 and 10 keV respectively. The pass energy of the analyzer was set at 70 eV for the Fisons apparatus and 50 eV for the Vacuum Generators XPS. The samples were measured without grinding of the CNF skeins.

3. Results and discussion

In Fig. 1A an SEM picture of an untreated CNF sample (CNF#1) is shown. The fibers with an average diameter of about 25 nm are interwoven, forming porous skeins in the micrometer range. The lighter spots in the image, two of them are indicated by arrows, are nickel particles from which the fibers had been grown. Fig. 2 displays a TEM image of untreated CNF (CNF#1), showing the individual sheets of the graphite-like lattice, ordered predominantly in the fishbone structure thus exposing the edges of the graphene layers [17]. In contrast to what might be concluded from this image, Ros et al. [18] mentioned that the ordering in the graphene sheets and their stacking in as-grown CNF is far from ideal. Regions of high defect concentrations alternate with defect-poor regions, which are presumably

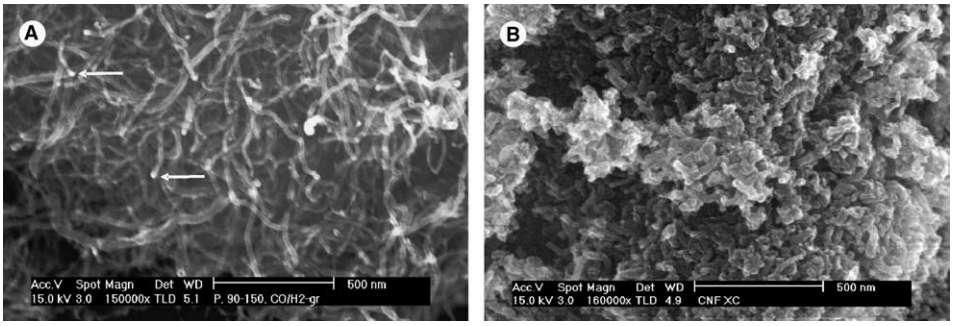

Fig. 1. SEM image of (A) CNF#1 and (B) CNF#6.

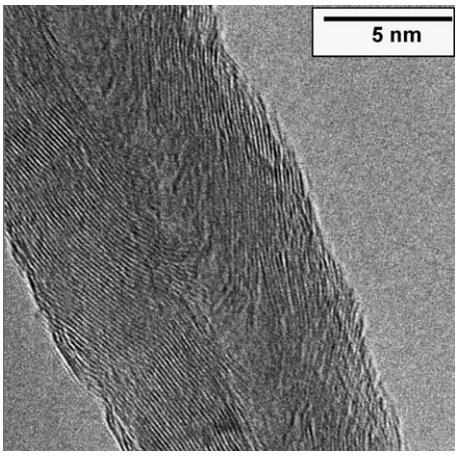

Fig. 2. TEM image of untreated carbon nanofibers (CNF#1).

more sensitive to oxidation. Also Nijkamp stated that untreated CNF display a significant amount of defects, such as two planes coinciding to one, bending planes, planes more or less parallel to the fiber axis and plane ends parallel to the fiber surface [19].

3.1. Graphite-like structure of carbon nanofibers

The effect of the various oxidation treatments on the graphite-like structure of all CNF samples has been studied using XRD and TEM. In Fig. 3 the diffraction patterns are shown. Untreated CNF#1 distinctly shows diffraction peaks of graphite-like carbon, next to diffraction peaks of nickel. These diffraction patterns demonstrate that the subsequent treatments in acid did not affect the integrity of the graphite-like structure, since the carbon peak positions and widths are unaltered. The set of patterns also demonstrates the removal of (part of the) nickel present after the growth of the fibers. TEM examination showed that graphitic envelopes encapsulate the remaining nickel. Moreover, TEM images of the samples (not shown) indicate that the characteristics of the CNF remained the same, i.e. the graphite-like structure is still intact and no change in average diameter is observed. So, both techniques prove that the graphite-like bulk structure was unaffected after the oxidation.

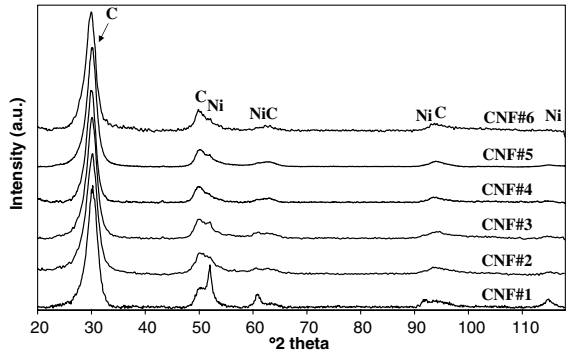

Fig. 3. X-ray diffraction patterns of untreated and treated carbon nanofibers.

3.2. Texture of carbon nanofibers

The textural properties of CNF#1 to #6 were investigated by means of nitrogen physisorption and SEM. Furthermore, the carbon burn-off percentage of the various acid treatments were measured, as listed in Table 1. Oxidizing CNF in HNO_3 or 1:1 HNO_3/H_2SO_4 (CNF#3 to #5) results in a weight loss of 2–4 wt.%, which can be chiefly explained by the removal of non-encapsulated nickel. Oxidation in 1:3 HNO_3/H_2SO_4 (CNF#6) for 0.5 h results in a considerable weight loss of 22%. This sample required a substantially longer filtration time than the other samples. Probably plugging of the 200 nm pores of the filter occurred. After treatment in this acid mixture for 2 h hardly any fibers remained.

The SEM images of CNF#2 to #4 are very similar to the SEM image of CNF#1 shown in Fig. 1A. The macroscopic structure of CNF#5 and especially that of CNF#6, however, is much more dense and the fibers are considerably shorter (Fig. 1B).

The weight loss and the SEM images after treatment in 1:3 HNO_3/H_2SO_4 display a partial destruction of the fibers. The original, mainly macroporous skeins of long and interwoven fibers had been converted into a more dense packing of short fiber fragments. Treatment in 1:1 HNO_3/H_2SO_4 also results in fragmentation, but to a significantly lower extent. This is confirmed by the much smaller weight loss upon treatment of CNF#5 compared to that of CNF#6. SEM images of the various samples show that the fragments have about the same average diameter as that of the untreated fibers, which strongly suggests that the original long fibers are broken up perpendicular to the length axis. Treatment of the fibers with a strong oxidizing agent ultimately leads to complete oxidation and consumption of defect-rich regions in the CNF, leaving the short fragments. Also other investigators have reported on the breaking up of MWNT [11,13,14,20] and SWNT [21] into smaller fragments by liquid-phase oxidation.

To obtain information on the effect of the pretreatment on the structure of the CNF, nitrogen physisorption experiments were performed on CNF#1 to #6. As representative examples, the adsorption isotherms of two CNF samples, one before and one after oxidation (CNF#2 and #5), are given in Fig. 4. The derived values of S_{BET}, total pore volumes and micropore volumes of all samples are summarized in Table 2. The isotherms are characteristic of multilayer adsorption/desorption accompanied by capillary condensation in relatively large mesopores, causing a hysteresis loop. The shape of

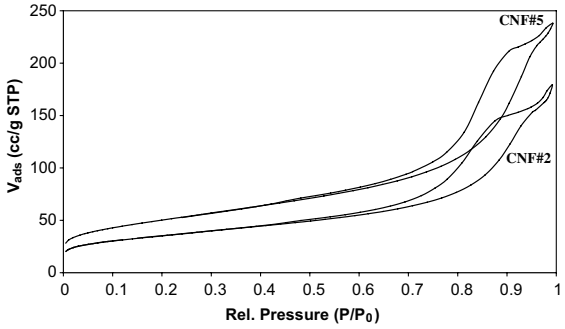

Fig. 4. Adsorption–desorption isotherm of N_2 of CNF#2 and CNF#5.

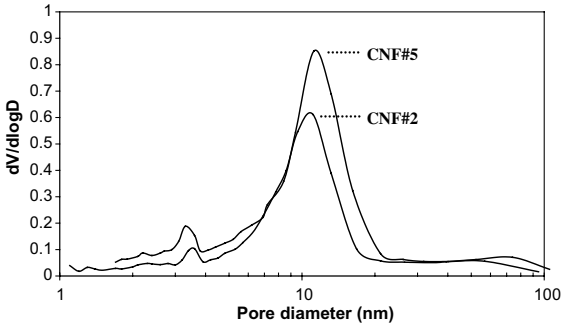

Fig. 5. Pore size distributions of CNF#2 and #5.

Table 2
Some physico-chemical features of carbon nanofibers before and after the various oxidation treatments

Samples	S_{BET} (m^2/g)	V_{pore} total (cm^3/g)
CNF#1	137[a]	0.21
CNF#2	138	0.25
CNF#3	156	0.30
CNF#4	186	0.36
CNF#5	183	0.38
CNF#6	194	0.32

[a] S_{BET} after correction for still present silica support is ~130 m^2/g.

the hysteresis loops indicates a distribution of cylindrical pores open at both sides. From the corresponding *t*-plots for all samples a very low micropore volume of 0.01 ml/g can be derived. An increase in the total surface area is noticed with increasing severity of the oxidation treatment roughly coinciding with a proportional increase in pore volume of the material, as can be seen in Table 2.

Corrected for the silica support, a specific surface area of 130 m^2/g can be calculated for non-treated CNF (CNF#1). With increasing oxidation time of the same acid and/or increasing the oxidation power of the acid, the surface area gradually rises to 194 m^2/g. The pore volume of CNF#1 to #5 increased from 0.21 to 0.38 cm^3/g. For CNF#6, however, a slightly lower pore volume was found. This decrease might be correlated with the strong fragmentation and the associated more dense packing of the fibers as demonstrated with SEM.

Samples CNF#1 up to #5 exhibited a relatively narrow pore size distribution with an average diameter of ≈12 nm. In Fig. 5 pore size distributions of CNF#2 and #5 are plotted as representative examples. Only with CNF#6 a somewhat broader pore diameter distribution was found with an average pore diameter of 8 nm. For the calculations of the pore size distributions the BJH (Barret–Joyner–Halenda) method has been applied, using the desorption branch of the nitrogen isotherms. Above ~4 nm diameter this method gives reliable pore size distributions based on the Kelvin equation, valid from 2 nm. However, in the 2–4 nm region artifacts can arise due to the closure of the hysteresis loop.

All oxidative treatments led to both an increase of specific surface area and pore volume, taking the respective values of CNF#2 as the base for comparison. The increase of specific surface area can be ascribed to three effects: fragmentation, surface roughening and opening of the inner tubes of the fibers. Fragmentation of the long fibers into shorter fragments of the same diameter hardly increases the specific surface. Taking into account the dimensions of the original fibers and that of the fragments as can be estimated from SEM images, we calculated that this effect is confined to about 10% in the case of CNF#6, the sample with the most and the shortest fragments.

Another explanation can be found in roughening of the fiber surface due to oxidative treatments. Shaikhutdinov et al. [22] earlier investigated the roughness of the surface of CNF. He utilized scanning tunneling microscopy (STM) to study the height differences on the surface of fishbone CNF and found considerable surface roughness factors of 4–5. The CNF used in our study presumably also have a rough surface. From the average diameter of the fibers of 25 nm an external surface area of 71 m^2/g can be derived, assuming a carbon density of 2.25 g/cm^3 and closed fibers. For CNF#2 a S_{BET} of 138 m^2/g is found and for CNF#6, the most oxidized CNF, 194 m^2/g. This implies that the surface area is 2–3 times larger than one would expect. From TEM, however, no evidence for enhanced surface roughness of the oxidized samples has been observed. Since only a small increase in surface area is observed from CNF#1 to CNF#2, it can be concluded that the changes in texture are not caused by the KOH treatment but can be ascribed to the treatment in oxidizing acids.

As most likely explanation for the increased surface area due to oxidation, opening of the inner tubes of the fibers remains. From literature it is known that MWNT can be opened by boiling them in oxidizing acids, thereby making their inner tubes accessible [11,13, 14,20]. If CNF are oxidized extensively, the nickel

particles on top of the fibers might be extracted and carbon from the center of the fiber can be removed, which could result in the formation of an inner tube with a diameter of several nanometers. Moreover, the fibers can be broken up at defect-rich areas, leading to opening of the fiber fragments. An argument that strongly supports this explanation is that a significant increase in pore volume is found going from sample CNF#1 to CNF#5 (Table 2) along with a proportional increase in surface area.

The difference in total pore volume of CNF#5 and CNF#2 is 0.13 cm^3/g. Calculations using an average fiber diameter of 25 nm and an average inner tube diameter of 12 nm, taken from the pore size distribution plots, show that opening of ~65% of the CNF can give rise to this increase in pore volume, while an increase in surface area of 43 m^2/g has to be expected. A difference in S_{BET} between CNF#5 and CNF#2 of 45 m^2/g was found with nitrogen physisorption (Table 2). These calculations support the supposition that opening of part of the inner tubes of CNF upon oxidation occurs.

From the adsoption–desorption isotherms it was concluded that filling of cylindrical pores very likely caused the hysteresis. Cylindrical pores indeed suggest the opening of the CNF, while between the fibers the pores are far from cylindrical. At first sight, the fact that no significant changes in the pore size distributions of CNF#2 to CNF#5 are found, while the majority of the inner tubes become accessible, is surprising. This might be explained by assuming that at maximum 35% of the CNF#2 fibers is already accessible for N_2-physisorption.

Studies of our group on the deposition of metals on CNF convincingly provide proof for the opening of the fibers. TEM tilt series have shown that part of the metal (Ni, Pd, Co) can be deposited in the inner tubes of oxidized CNF. [1]

3.3. Number of oxygen-containing surface groups

A direct acid–base titration technique using NaOH was performed to determine the number of surface groups exhibiting a $pK_a < 7.5$. Titration curves obtained with samples CNF#3 and #6 are displayed as examples in Fig. 6. In Table 3 the numbers of acidic oxygen-containing surface groups of the different samples as measured by titration are given. CNF#1 and #2 could not be measured reliably. Since these samples were too hydrophobic they could not be dispersed in water properly. The titration experiments demonstrate that an increase in severity of the oxidation results in an increase in the number of acidic surface sites, from 1.0 on CNF#3 to 3.3 acidic groups/nm^2 on CNF#6. Assuming

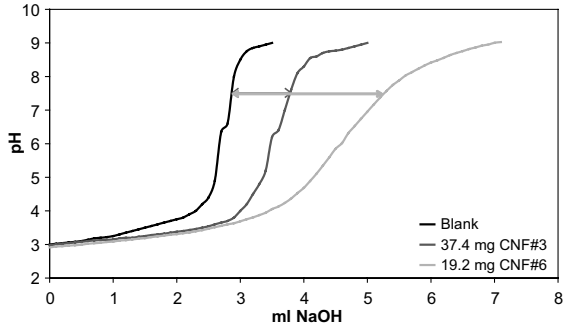

Fig. 6. Titration curves of CNF#3 and CNF#6.

that all acidic oxygen-groups are carboxylic groups the number of oxygen atoms/nm^2 is also calculated (Table 3).

XPS measurements were done to establish the amount of oxygen in the sub-surface (2–3 nm) of the CNF. In Table 3 the O/C atomic ratios of most of the CNF samples are given. Results obtained with this technique confirm an increase in oxygen concentration with increasing severity of the oxidation treatment. Part of the oxygen present in CNF#1 must be due to the presence of silica from the growth catalyst in this sample. However, in CNF#2 the silica has been removed meaning that the O/C ratio of 0.023 as found demonstrates that non-oxidized CNF do already contain some oxygen, probably taken up during the fiber growth from CO/H_2 or is due to reaction with oxygen or water during storage. The O/C ratios are converted to oxygen atoms/nm^2 using a model of Gijzeman. [2] The error in the numbers is estimated to be about 15%. These results (Table 3) show that fibers oxidized in HNO_3 for 2 h (CNF#4) contain 9.6 O atoms/nm^2. This implies that ca 5–10 oxygen-containing groups are present per nm^2, which is rather high. Values up to 1–3 groups/nm^2, as we found by titration, seem to be much more realistic [6]. An explanation for this discrepancy can be found by assuming that oxygen atoms are not present solely at the exterior surface, but also are built in the sub-surface of the fibers [7,23].

TGA-MS was used to study the amount of oxygen in the bulk as well as at the surface of the CNF samples. The total weight loss up to 1123 K is related to the total amount of oxygen present in the CNF and from the mass signals as function of the temperature information about the types of surface groups can be obtained. In Fig. 7 typical TGA-MS temperature patterns of CNF#1 and CNF#5 are displayed. Weight loss of the untreated sample CNF#1 is relatively small, about 1%, as can be

[1] Winter F, Bezemer GL, van der Spek C, Meeldyk GD, van Dillen AJ, de Jong KP. to be published.

[2] More information about this model can be obtained from O.L.J. Gijzeman, Department of Inorganic Chemistry and Catalysis Utrecht University, Sorbonnelaan 16, P.O. Box 80083, 3508 TB Utrecht, The Netherlands.

Table 3
Titration, XPS and TGA-MS (corrected for phys. water) results of carbon nanofibers after different treatments

Samples	Titration		TGA-MS		XPS	
	Acidic oxygen-containing surface groups/nm^2 ($pK_a \leqslant 7.5$)	O atoms/nm^2	Weight loss (%)	O atoms/nm^2	O/C atomic ratio	O atoms/nm^2
CNF#1	–	–	<0.5	<1.2 ± 0.2	0.016	2.3 ± 0.3
CNF#2	–	–	–	–	0.023	3.4 ± 0.5
CNF#3	1.0 ± 0.1	2.0 ± 0.2	4.0	8.3 ± 0.6	–	–
CNF#4	1.4 ± 0.1	2.8 ± 0.2	5.7	9.8 ± 0.8	0.069	9.6 ± 1.4
CNF#5	1.5 ± 0.2	3.0 ± 0.4	6.4	9.8 ± 0.8	–	–
CNF#6	3.3 ± 0.3	6.6 ± 0.6	9.2	12.3 ± 1.1	–	–
CNF#4 573 K N_2	1.0 ± 0.1	2.0 ± 0.2	3.7	6.3 ± 0.5	0.038	5.3 ± 0.8
CNF#4 773 K N_2	0.2 ± 0.02	0.4 ± 0.04	3.3	5.6 ± 0.5	0.032	4.4 ± 0.7
CNF#4 973 K N_2	~0.03 ± 0.003	~0.06 ± 0.006	1.8	3.0 ± 0.3	0.017	2.3 ± 0.3

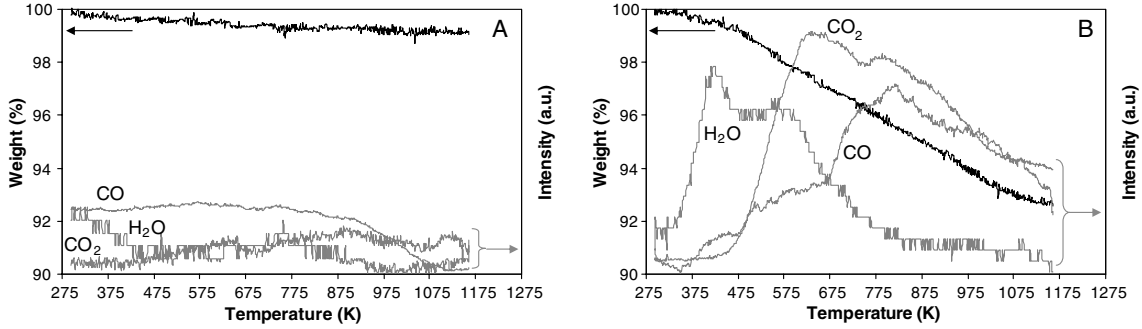

Fig. 7. TGA-MS patterns in Ar. (A) CNF#1 and (B) CNF#5.

seen in Fig. 7A. Only small amounts of H_2O, CO and CO_2 are formed during heating, meaning that untreated hydrophobic CNF (CNF#1) contain small amounts of thermally removable oxygen and physisorbed water.

From Fig. 7B it is evident that due to the treatment in 1:1 HNO_3/H_2SO_4 substantial amounts of oxygen had been taken up in CNF#5. Up to 1123 K a total weight loss of 7.5% was measured, which confirms the results of Ros et al. [7] obtained with oxidized CNF and MWNT. The TGA-MS patterns of CNF#4 and CNF#6 are very similar to that of CNF#5 (Fig. 7B), is it that the total weight losses increase from CNF#1 to #6.

From the literature it is known that the water peak around 423 K can be ascribed to evolved physisorbed water [7,24]. The second peak at 523 K might originate from carboxylic anhydrides formed from neighboring carboxyl groups. CO_2 evolution around 623 K is attributed to the decomposition of carboxylic groups [6,7,24,25] and CO_2 evolving at still higher temperatures originates from carboxylic anhydrides and/or lactones [7,24–26]. For the CO evolution profile the assignment is less certain. CO could originate amongst others from phenol, carbonyl, quinone, ether and anhydride groups [7,8,24,25].

TGA-MS demonstrates that treatment of the fibers in HNO_3 for 0.5 h, CNF#3, already results in the formation of a significant amount of oxygen-containing groups. However in the CO and CO_2 patterns no distinct maxima are measured making assignment difficult. Weight loss profiles of CNF#4 up to #6 are very alike and discussed together. The CO_2 patterns demonstrate the presence of carboxyl and anhydride groups on their surface, decomposing from ~473 to 750 K and higher temperatures.

Water evolved preceding the CO and CO_2 evolution, arises from physisorbed water. To enable quantification of the loss of weight due to evolution of oxygen-containing compounds, weight loss due to removal of physisorbed water should be subtracted from the total weight loss. The corrected weight losses of all CNF samples are listed in Table 3. It may be concluded that weight loss is related to the severity of the oxidation treatment. With CNF#1 a weight loss of <0.5% was found, while for the oxidized samples CNF#3 to #6 weight losses of 4.0%, 5.7%, 6.4% and 9.2% were measured respectively. When it is assumed (see [7]) that CO and CO_2 evolve in a ratio of 1:1, that weight loss exclusively originates from decomposition of oxygen

groups, and the BET surface areas are taken, the number of oxygen atoms/nm^2 can be calculated. The results are given in Table 3. The error margins are estimated by assuming CO/CO_2 ratios of 1:2 and 2:1. Untreated CNF (CNF#1) contains <1.2 oxygen atoms/nm^2. Dependent on the severity of the oxidation treatment 8.3–12.3 oxygen atoms/nm^2 are found. As discussed earlier concerning our XPS results it is not likely that all these groups are localized at the surface. Probably oxygen is also built in the sub-surface of the fibers [7,23]. Our results are in agreement with values found in literature. Hoogenraad [2] found a weight loss of more than 10% for CNT treated in HNO_3 for 2 h and Ros et al. [7] found weight losses up to 7% for oxidized CNF.

With titration, XPS and with TGA-MS we found an increase in the amount of oxygen with the severity of the oxidation treatment. Using titration, the lowest numbers are found, because with this technique only the acidic groups ($pK_a < 7.5$) at the exterior surface can be measured. The number of oxygen atoms as determined using XPS and TGA-MS are comparable when the error margins are taken into account. From this we can conclude that besides acidic groups on the CNF surface, oxygen is built in the outer 2–3 nm of the fibers and no significant amounts of oxygen are incorporated in the bulk of the CNF during oxidation. It is also likely that some non-acidic groups are present on the surface of the CNF.

3.4. Thermostability of oxygen-containing surface groups

To study the thermal stability of the acidic oxygen-containing surface groups CNF#4 was heat-treated in flowing N_2 at 573, 773 and 973 K for 2 h. The results as given in Table 3 show a decrease of the number of acidic groups/nm^2 as determined using acid–base titrations, from 1.4 to respectively 1.0, 0.2 and 0.03 after heat treatment at the respective temperatures. These results show that only a small part of the acidic groups decomposes below 573 K. After treatment at 773 K, the majority of the acidic groups had been removed from the surface. This is in accordance with our TGA-MS results, showing that the decomposition of the carboxylic groups occurred in the range 473–750 K. Treatment in nitrogen at 973 K eliminated almost all acidic oxygen-containing groups from the surface. In the literature it is reported that below this temperature acid sites are destroyed and basic surface oxides can be formed when the carbon surface comes into contact with air after cooling [4–6,8].

In Table 3 also the oxygen contents of the heat-treated samples as measured with XPS and TGA-MS are given. With both techniques a gradual decrease in the oxygen amount with temperature was observed. The numbers indicate that part of the oxygen is easily removed, since after treatment at 573 K a significant part of the oxygen atoms/groups had been removed. Most interesting is that TGA-MS results indicate that after treatment at 973 K for 2 h 3.0 oxygen atoms/nm^2 remained and with XPS it was found that 2.3 oxygen atoms/nm^2 survived this heat treatment. This shows that some very thermostable oxygen is present and/or new basic surface oxides are formed upon exposure to oxygen. These groups might play an important role in the prevention of sintering of metal particles in CNF-supported catalysts at high temperatures [27].

4. Conclusions

Small diameter fishbone carbon nanofibers (CNF) ($Ø \sim 25$ nm) were oxidized in HNO_3 and mixtures of HNO_3/H_2SO_4 for 0.5 and 2 h. Results demonstrate that the graphite-like structure had remained intact after the different oxidation treatments. However, the texture of the CNF is significantly altered. Specific surface area and pore volume increased with the severity of the treatment. We have shown that these changes in texture are mainly due to opening of the inner tubes of the CNF.

Furthermore, we showed that both the total oxygen content and the number of acidic oxygen-containing surface groups can be tuned by variation of the treatment time and by the type of acid or acid mixture used. Besides acidic oxygen groups (1–3 groups/nm^2) at the CNF exterior surface that are formed upon oxidation, also oxygen is built in the first 2–3 nm of the sub-surface of the fibers.

Treatment of CNF oxidized in HNO_3 for 2 h in inert atmosphere at 973 K leads to almost complete decomposition of the acidic oxygen-containing groups. However, non-acidic oxygen groups/nm^2 are still present on/in the CNF, showing that some very thermostable oxygen remains and/or new basic surface oxides are formed upon exposure to air.

Acknowledgements

The authors are grateful to C. van der Spek for operating the TEM, M. Versluijs-Helder for the SEM images, A. Broersma for the TGA-MS experiments, G.L. Bezemer for the burn-off experiments and A.J.M. Mens for the N_2-physisorption and XPS measurements. We also thank Shell International B.V. for the XPS measurements. Prof. Dr. M.R. Egmond and R. Dijkman of the Department Membrane Enzymology are acknowledged for their help with the acid–base titrations.

These investigations are supported by the Council for Chemical Sciences of the Netherlands Organization for

Scientific Research with financial aid from the Netherlands Technology Foundation (CW/STW 349-5357).

References

[1] de Jong KP, Geus JW. Catal Rev-Sci Eng 2000;42:482–510.
[2] Hoogenraad MS. Utrecht University NL, PhD Thesis, 1995.
[3] Toebes ML, Bitter JH, van Dillen AJ, de Jong KP. Catal Today 2002;76:33–42.
[4] Rodriguez-Reinoso F. Carbon 1998;36:159–75.
[5] Jansen RJJ. Delft University NL, PhD Thesis, 1994.
[6] Boehm HP. Adv Catal 1966;16:179–264.
[7] Ros TG, van Dillen AJ, Geus JW, Koningsberger DC. Chem Eur J 2002;8:1151–62.
[8] Boehm HP. Carbon 2002;40:145–9.
[9] Vogel AI. Textbook of practical organic chemistry. London: Longman, Green and Co.; 1957. p. 523–5.
[10] Edwards HGM, Fawcett V. J Mol Struct 1994;326:131–43.
[11] Hiura H, Ebbesen TW, Tanigaki K. Adv Mater 1995;7:275–6.
[12] Chattopadhyay D, Galeska I, Papadimitrakopoulos F. Carbon 2002;40:985–8.
[13] Tsang SC, Chen YK, Harris PJF, Green MLH. Nature 1994; 372:159–62.
[14] Li Y-H, Wang S, Luan Z, Ding J, Xu C, Wu D. Carbon 2003;41:1057–62.
[15] Darmstadt H, Summchen L, Ting J-M, Roland U, Kaliaguine S, Roy C. Carbon 1997;35:1581–5.
[16] van Dillen AJ, Geus JW, Hermans LAM, van der Meijden J. Stud Surf Sci Catal 1977;2:677–84.
[17] Rodriguez NM, Chambers A, Baker RTK. Langmuir 1995; 11(10):3862–6.
[18] Ros TG, van Dillen AJ, Geus JW, Koningsberger DC. Chem Phys Chem 2002;3:209–14.
[19] Nijkamp M. Utrecht University NL, PhD Thesis, 2002.
[20] Li C-H, Yao K-F, Liang J. Carbon 2003;41(4):858–60.
[21] Liu J, Rinzler AG, Dai H, Hafner JH, Bradley RK, Boul PJ, et al. Science 1998;280:1253–6.
[22] Shaikhutdinov ShK. Kinet Catal 1995;36:549–606.
[23] He H, Klinowski J, Fortser M, Lerf A. Chem Phys Lett 1998; 287:53–6.
[24] Haydar S, Moreno-Castilla C, Ferro-Garcia MA, Carrasco-Marin F, Rivera-Utrilla J, Perrard A, et al. Carbon 2000;38: 1297–308.
[25] Aksoylu AE, Madalena M, Freitas A, Fernando M, Pereira R, Figueiredo JL. Carbon 2002;39:175–85.
[26] Domingo-García M, López Garzón FJ, Pérez-Mendoza MJ. J Coll Inter Sci 2002;248:116–22.
[27] Toebes ML, Prinsloo FF, Bitter JH, van Dillen AJ, de Jong KP. J Catal 2003;214:78–87.